

See discussions, stats, and author profiles for this publication at: <https://www.researchgate.net/publication/47386470>

Expression of Chirality and Visualization of Stereogenic Centers by Scanning Tunneling Microscopy

ARTICLE *in* LANGMUIR · APRIL 1999

Impact Factor: 4.46 · DOI: 10.1021/la9811057 · Source: OAI

CITATIONS

53

READS

13

8 AUTHORS, INCLUDING:



Steven De Feyter

University of Leuven

326 PUBLICATIONS 9,691 CITATIONS

SEE PROFILE



Frans C De Schryver

University of Leuven

670 PUBLICATIONS 21,267 CITATIONS

SEE PROFILE



Suresh Valiyaveetil

National University of Singapore

232 PUBLICATIONS 6,673 CITATIONS

SEE PROFILE

Expression of Chirality and Visualization of Stereogenic Centers by Scanning Tunneling Microscopy

S. De Feyter, A. Gesquière, P. C. M. Grim, and F. C. De Schryver*

Laboratory of Molecular Dynamics and Spectroscopy, Department of Chemistry, University of Leuven (KU Leuven), Celestijnenlaan 200-F, 3001 Heverlee, Belgium

S. Valiyaveetil, C. Meiners, M. Sieffert, and K. Müllen

Max-Planck Institute for Polymer Research, P.O. Box 3148, D-55021 Mainz, Germany

Received August 25, 1998. In Final Form: December 21, 1998

Physisorbed monolayer films of both enantiomers of a chiral terephthalic acid derivative, 2,5-bis[[10-(2-methylbutoxy)decyl]oxy]terephthalic acid, have been characterized on graphite (HOPG) at the solution–substrate interface using scanning tunneling microscopy (STM). The monolayers, which are imaged with submolecular resolution, are enantiomorphous. The adlayer consists of a lamellar structure in which two distinct lamellar widths can be identified. The lamellar width can be directly related to the length of that part of the molecule which is adsorbed on the graphite surface. In the narrow lamellae, the 2-methylbutoxy groups point away from the surface, giving rise to specific features in the STM image. These features can be described as discontinuous, elongated spots and appear also at the positions of the stereogenic centers. Because of the presence of the methyl group at the stereogenic center, the tunneling current is locally modulated, enabling the visualization of the stereogenic center.

Introduction

Self-organized monomolecular adlayers have been studied with scanning tunneling microscopy (STM) for a wide range of organic compounds.¹ A detailed discussion on the origin of the image contrast of substituted alkanes has been made by Claypool et al. and Faglioni et al.² The influence of molecular conformation on the two-dimensional organization of organic compounds on surfaces has already been studied with atomic force microscopy (AFM) and STM. Specifically, using STM, Rabe et al. observed a gauche conformation of the central disulfide bridge of dihexadecyl disulfide, which is reflected by a V shape of the individual molecules.³ Within our research group the cis–trans isomerization of azobenzene derivatives was studied at the liquid–graphite interface.⁴ Cyr et al. imaged monolayer films of 1-bromodocosane on graphite and reported a contrast variation over time related to a conformational change.⁵ Conformational analysis of porphyrin derivatives was reported by Jung et al.⁶ These investigations reveal the applicability of STM in the study of molecular conformation.

Chiral segregation in Langmuir–Blodgett films has been reported using AFM by Eckhardt et al.⁷ Enantiomorphous monolayer formation of liquid-crystalline enantiomers at the graphite surface⁸ as well as the expression of chirality by achiral coadsorbed molecules in chiral monolayers consisting of chiral isophthalic acid derivatives was visualized by STM.⁹ Recently, Lopinski et al. have reported the determination of the absolute chirality of individual adsorbed alkenes chemisorbed on the silicon(100) surface using STM.¹⁰

These studies show that STM can identify molecular conformation and chirality at the submolecular level. We would like to advance this one step further by demonstrating that we have succeeded in not only observing enantiomorphous monolayer crystals from the enantiomers of a terephthalic acid derivative but also visualizing the stereogenic centers, analyzing chirality and conformation simultaneously at the liquid–graphite interface.

Experimental Section

(S)-2,5-Bis- and (R)-2,5-bis[[10-(2-methylbutoxy)decyl]oxy]terephthalic acids ((S)- and (R)-**1**) were prepared from the corresponding enantiomers of 2-methyl-1-butanol. (R)-2-Methyl-1-butanol was obtained from (R)-2-methyl-1-butanolic acid¹¹ (*er R:S* ≈ 92:8, determined by GC and the optical rotation) under

* To whom correspondence should be addressed.

(1) (a) McGonigal, G. C.; Bernhardt, R. H.; Thomson, D. J. *Appl. Phys. Lett.* **1990**, *57*, 28–30. (b) Frommer, J. *Angew. Chem.* **1992**, *104*, 1325; *Angew. Chem., Int. Ed. Engl.* **1992**, *31*, 1298–1328. (c) Rabe, J. P.; Buchholz, S. *Science* **1991**, *253*, 424–427. (d) Cyr, D. M.; Venkataraman, B.; Flynn, G. W. *Chem. Mater.* **1996**, *8*, 1600–1615.

(2) (a) Claypool, C. L.; Faglioni, F.; Goddard, W. A., III; Gray, H. B.; Lewis, N. S.; Marcus, R. A. *J. Phys. Chem. B* **1997**, *101*, 5978–5995. (b) Faglioni, F.; Claypool, C. L.; Lewis, N. S.; Goddard, W. A., III. *J. Phys. Chem. B* **1997**, *101*, 5996–6020.

(3) Rabe, J. P.; Buchholz, S.; Askadskaya, L. *Synth. Met.* **1993**, *54*, 339–349.

(4) (a) Grim, P. C. M.; Vanoppen, P.; Rücker, M.; De Feyter, S.; Valiyaveetil, S.; Moessner, G.; Müllen, K.; De Schryver, F. C. *J. Vac. Sci. Technol. B* **1997**, *15*, 1419–1424. (b) Vanoppen, P.; Grim, P. C. M.; Rücker, M.; De Feyter, S.; Moessner, G.; Valiyaveetil, S.; Müllen, K.; De Schryver, F. C. *J. Phys. Chem.* **1996**, *100*, 19636–19641.

(5) Cyr, D. M.; Venkataraman, B.; Flynn, G. W.; Black, A.; Whitesides, G. M. *J. Phys. Chem.* **1996**, *100*, 13747–13759.

(6) Jung, T. A.; Schlittler, R. R.; Gimzewski, J. K. *Nature* **1997**, *386*, 696–698.

(7) Eckhardt, C. J.; Peachy, N. M.; Swanson, D. R.; Takacs, J. M.; Khan, M. A.; Gong, X.; Kim, J.-H.; Wang, J.; Uphaus, R. A. *Nature* **1993**, *362*, 614–616.

(8) (a) Stevens, F.; Dyer, D. J.; Walba, D. M. *Angew. Chem.* **1996**, *108*, 955–957; *Angew. Chem., Int. Ed. Engl.* **1996**, *35*, 900–901. (b) Walba, D. M.; Stevens, F.; Clark, N. A.; Parks, D. C. *Acc. Chem. Res.* **1996**, *29*, 591–597.

(9) De Feyter, S.; Grim, P. C. M.; Rücker, M.; Vanoppen, P.; Meiners, C.; Sieffert, M.; Valiyaveetil, S.; Müllen, K.; De Schryver, F. C. *Angew. Chem.* **1998**, *110*, 1281–1284; *Angew. Chem., Int. Ed. Engl.* **1998**, *37*, 1223–1226.

(10) Lopinski, G. P.; Moffatt, D. J.; Wayner, D. D.; Wolkow, R. A. *Nature* **1998**, *392*, 909–911.

(11) Freudenberg, K.; Lwowski, W. *Justus Liebigs Ann. Chem.* **1955**, *594*, 76.

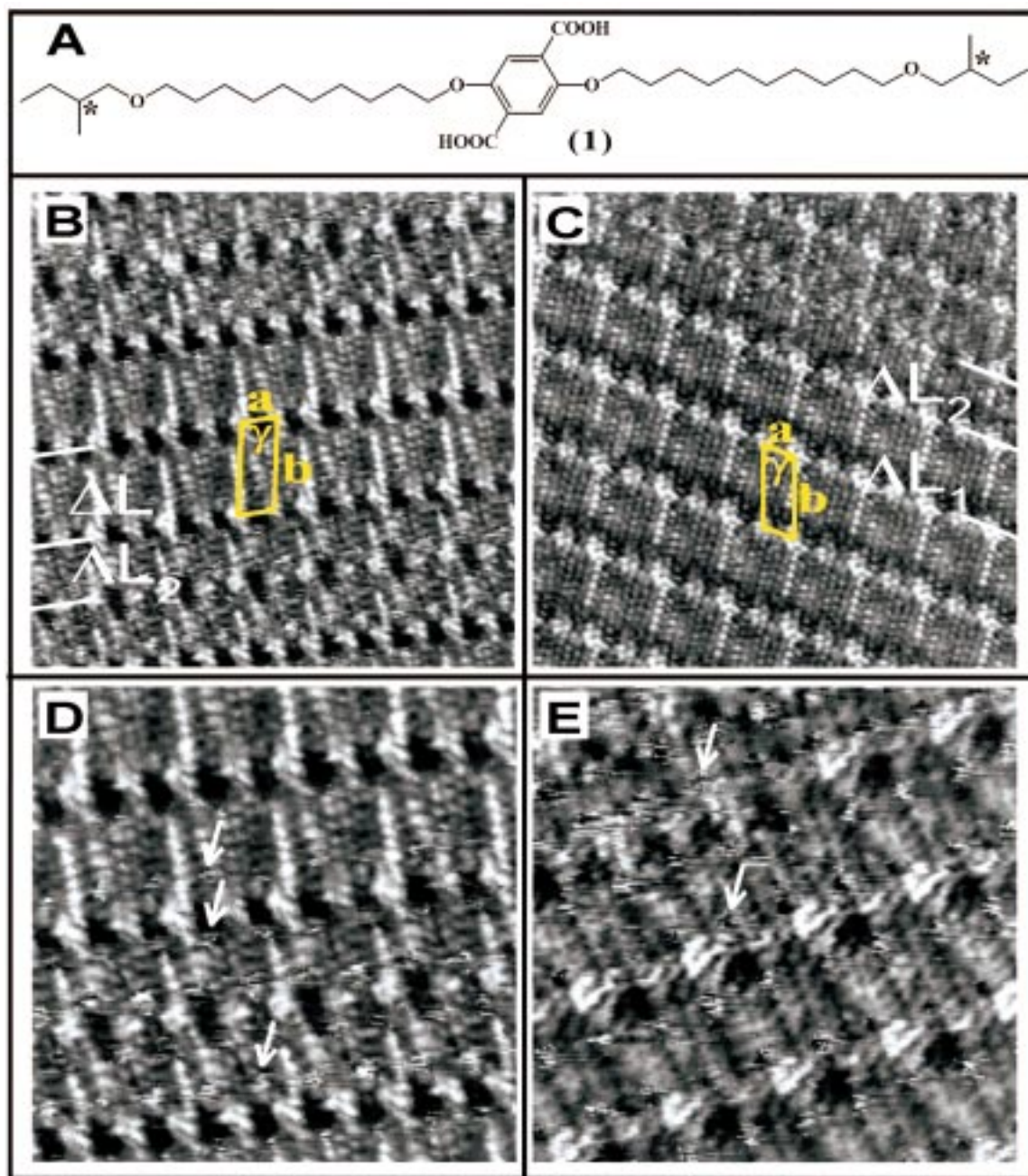


Figure 1. (A) Chemical structure of 5-[[10-(2-methylbutoxy)decyl]oxy]terephthalic acid (**1**). The stereogenic centers are indicated by an asterisk. (B) STM image of an ordered monolayer of (*S*)-**1** molecules formed by physisorption at the 1-phenyloctane–graphite interface. The image size is $11.7 \times 11.7 \text{ nm}^2$. $I_{\text{set}} = 0.5 \text{ nA}$, and $V_{\text{bias}} = -0.62 \text{ V}$. (C) STM image of an ordered monolayer of (*R*)-**1** molecules. The image size is $11.7 \times 11.7 \text{ nm}^2$. $I_{\text{set}} = 1.0 \text{ nA}$, and $V_{\text{bias}} = -0.47 \text{ V}$. ΔL_1 and ΔL_2 are respectively the large and small spacings between two adjacent rows of terephthalic acid groups. The two-dimensional unit cell of the monolayer structure composed of wide lamellae is presented (indicated in yellow). The lamellar axes in parts B and C make angles θ of respectively $-3.7 \pm 0.3^\circ$ and $+3.7 \pm 0.3^\circ$ with the normal on that particular graphite axis which is in registry with the alkoxy chains. (D) STM image of a (*S*)-**1** monolayer. The image size is $7.8 \times 7.8 \text{ nm}^2$. $I_{\text{set}} = 0.5 \text{ nA}$, and $V_{\text{bias}} = -0.62 \text{ V}$. (E) STM image of a (*R*)-**1** monolayer. The image size is $7.8 \times 7.8 \text{ nm}^2$. $I_{\text{set}} = 0.4 \text{ nA}$, and $V_{\text{bias}} = -0.37 \text{ V}$. The arrows indicate some of the discontinuous streaky features which are related to the presence of stereogenic centers (wide lamellae) or with the 2-methylbutoxy groups bent away from the surface (narrow lamellae).

retention of configuration as described in ref 12. (*S*)-2-Methyl-1-butanol was purchased from Fluka (*er S*:*R* \approx 99:1, determined by GC). The optical purity of the enantiomers was checked by optical rotation. (*S*)-**1**: $[\alpha]_{\text{D}}^{23} \approx +0.8$ ($c = 3.6$ in THF); (*R*)-**1**: $[\alpha]_{\text{D}}^{23} \approx -0.8$ ($c = 3.0$ in THF). The optical purity of the enantiomers of **1** is based upon the optical purity of the (*S*)- and (*R*)-2-methylbutanol used, as it was proven that retention of the configuration is maintained. Therefore, (*S*)-**1**, bearing two *S*

centers, was prepared in approximately 98% purity. (*R*)-**1**, containing two *R* centers, was prepared in approximately 85% purity.

2,5-Bis[(10-butoxydecyl)oxy]terephthalic acid (**2**) was synthesized from butanoic acid. The consequent preparative steps are analogous to those of compound **1**.

Prior to imaging, all compounds under investigation were dissolved in 1-phenyloctane (Aldrich, 99%), at a concentration of approximately 5 mg/mL, and a drop of this solution was applied on a freshly cleaved surface of highly oriented pyrolytic graphite.

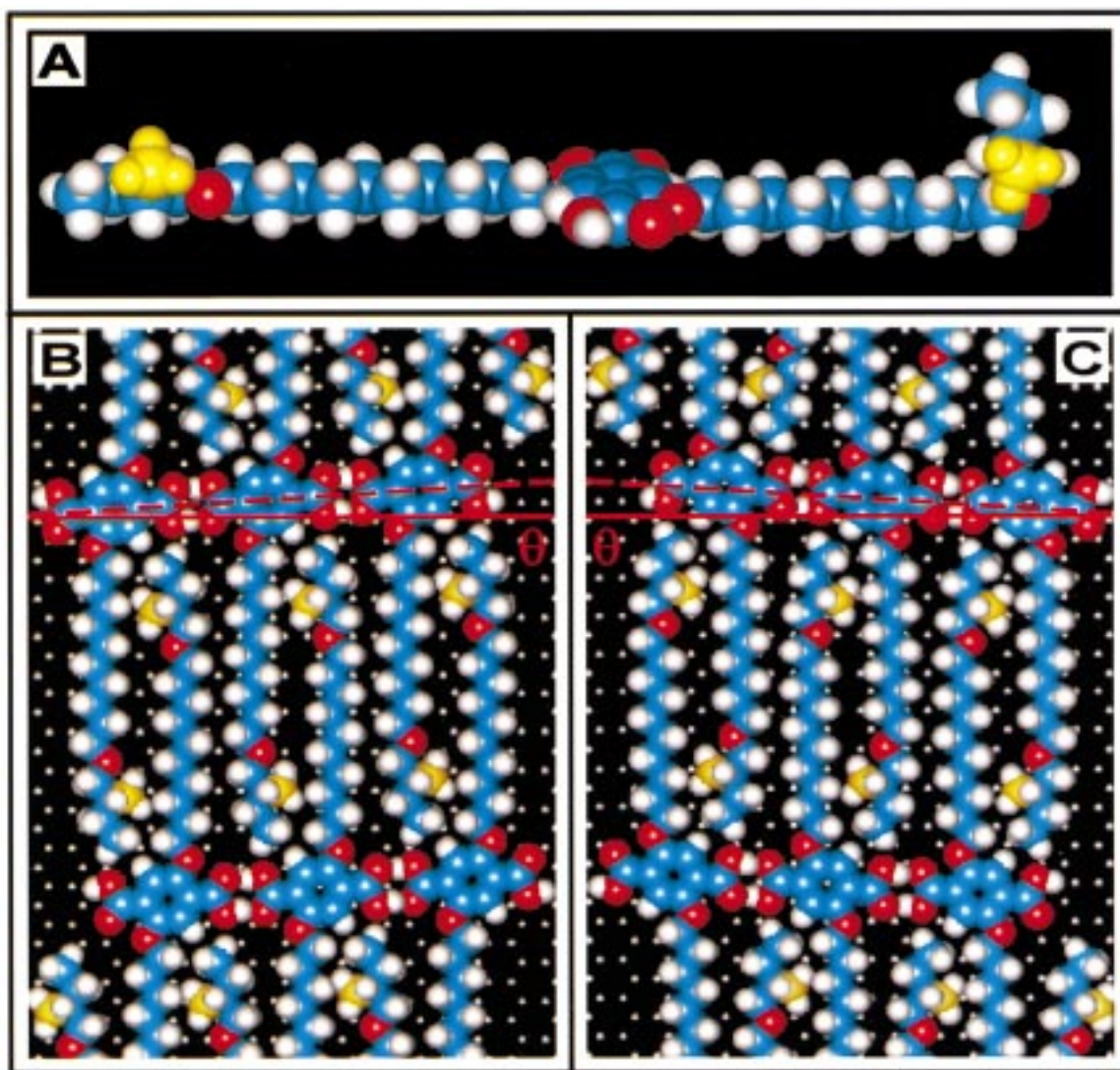


Figure 2. (A) Molecular model of (*S*)-**1**. At the left-hand side of the terephthalic acid moiety, the aliphatic chain is completely extended, as observed in wide lamellae. At the right-hand side of the terephthalic acid moiety, the terminal 2-methylbutoxy group is bent away, as occurs in the small lamellae. (B) Proposed molecular model for the molecular arrangement in adjacent wide lamellae of a domain composed of (*S*)-**1** molecules and (C) a domain composed of (*R*)-**1** molecules. θ is the angle between the lamellar axis (red dashed line) and the normal on that particular graphite axis which is in registry with the alkoxy chains (red line). Blue = carbon, red = oxygen, white = hydrogen, and yellow is the carbon atom of the methyl group on the stereogenic center. The small white spots are the carbon atoms of the graphite surface.

The STM images were acquired in the variable-current mode (constant height) under ambient conditions, unless otherwise stated in the text. In the STM images, white corresponds to the highest and black to the lowest measured tunneling current. STM experiments were performed using a Discoverer scanning tunneling microscope (Topometrix Inc., Santa Barbara, CA) along with an external pulse/function generator (model HP 8111 A), with negative sample bias. Tips were electrochemically etched from a Pt/Ir wire (80%/20%, diameter 0.2 mm) in a 2 N KOH/6 N NaCN solution in water.

The experiments were repeated in several sessions using different tips to check for reproducibility and to avoid artifacts. Different settings for the tunneling current and the bias voltage were used, ranging from 0.3 to 1.0 nA and from -10 mV to -1.5 V, respectively. The unit cell parameters were not affected by the difference in experimental conditions. After registration of a STM image of a monolayer structure, the underlying graphite surface was recorded at the same position by decreasing the bias voltage, serving as an in situ calibration.

Results and Discussion

A chiral terephthalic acid derivative, 2,5-bis[[10-(2-methylbutoxy)decyl]oxy]terephthalic acid (**1**) (Figure 1A),

bearing two stereogenic centers, was allowed to form chiral physisorbed monolayers on a graphite surface. Both tetrahedral stereogenic centers are indicated by an asterisk. Parts B and C of Figure 1 represent STM images of physisorbed monolayer structures of respectively (*S*)- and (*R*)-**1**. Both images reveal a closely packed arrangement of molecules on the graphite surface with sub-molecular resolution. The aromatic terephthalic acid groups appear as the larger bright spots. Rows of adjacent terephthalic acid groups are marked by white lines. Two different spacings are found between adjacent rows of (*R*)- or (*S*)-**1** terephthalic acid groups. For both enantiomers, the width of the wide lamellae ($\Delta L_1 = 2.54 \pm 0.05$ nm)—a lamella is defined as the region between two adjacent rows of terephthalic acid groups—corresponds to the dimension of fully extended alkoxy chains, which are lying flat on the graphite surface. The alkoxy chains make an angle of $2 \pm 1^\circ$ with respect to the nearest main graphite axis. The width of the narrow lamellae ($\Delta L_2 = 1.90 \pm 0.10$ nm) is in good agreement with the distance between the terephthalic acid group and the oxygen atom in the alkoxy

chain. We therefore conclude that part of the chain, namely, the 2-methylbutoxy group, is bent away from the surface, while the decyloxy groups are lying flat on the graphite surface, adopting an all-trans conformation. Stevens et al. reported on lamellar structures in which short alkoxy chains are bent away from the surface.¹³ Recently, a similar observation has been documented by Gorman et al. for one of the alkyl chains of 5-(*N,N*-didecylamino)-2,4-pentadienal.¹⁴ In Figure 2A, a molecular model is presented which reflects the two described conformations of the chains. At the left-hand side of the terephthalic acid moiety, the aliphatic chain is completely extended. At the right-hand side of the terephthalic acid moiety, the terminal 2-methylbutoxy group is bent away. Wide and narrow lamellae coexist in the same mixed phase. Three situations are possible: (1) all alkoxy chains of a row of **1** are extended, giving rise to two adjacent wide lamellae, (2) the alkoxy chains at only one side of a row of **1** are extended, leading to one wide lamella and an adjacent narrow lamella, and (3) all 2-methylbutoxy groups of a row of **1** are bent off the surface, giving rise to two adjacent narrow lamellae. In all cases, the alkoxy chains of adjacent rows of **1** are interdigitated. All arrangements mentioned are observed in Figure 1B.

The STM images exhibit a modulation of the contrast along the lamellae in both wide lamellae (ΔL_1) and narrow lamellae (ΔL_2). This is observed as a superstructure (Moiré pattern) along the lamellae with a repeat distance of four alkoxy chains. This superstructure is also observed for terephthalic acid groups within the same row for which the contrast varies in an alternating fashion. This modulation can be attributed to the fact that the monolayer structure is incommensurate with the underlying graphite lattice.^{1c,15} The Moiré pattern allows one to determine the intermolecular distance between alkoxy chains with high accuracy (0.48 nm).¹⁵ On the basis of this analysis, the center to center distance between adjacent terephthalic acid groups within the same row is 0.96 ± 0.01 nm. This distance is in good agreement with the value reported for the center to center distance of terephthalic acid units in a three-dimensional crystal (0.955 nm).¹⁶ The unit cells for both monolayer structures, indicated in yellow in parts B and C of Figure 1, are mirror images, which means that the enantiomers form enantiomorphous monolayer structures. The unit cell parameters are identical for both enantiomers.¹⁷

On the basis of the data analysis, a molecular model has been constructed of the two-dimensional organization of both enantiomers together with the underlying graphite surface (Figure 2B,C). Only the two-dimensional arrangement of molecules in adjacent wide lamellae is depicted here. The molecular model is made with the assumption that the methyl group on the stereogenic centers is not in contact with the graphite surface but is directed toward the solution phase. Evidence supporting the validity of this assumption is provided further in the text. The two-dimensional arrangement in narrow lamellae is similar, except for the terminal 2-methylbutoxy groups, which are

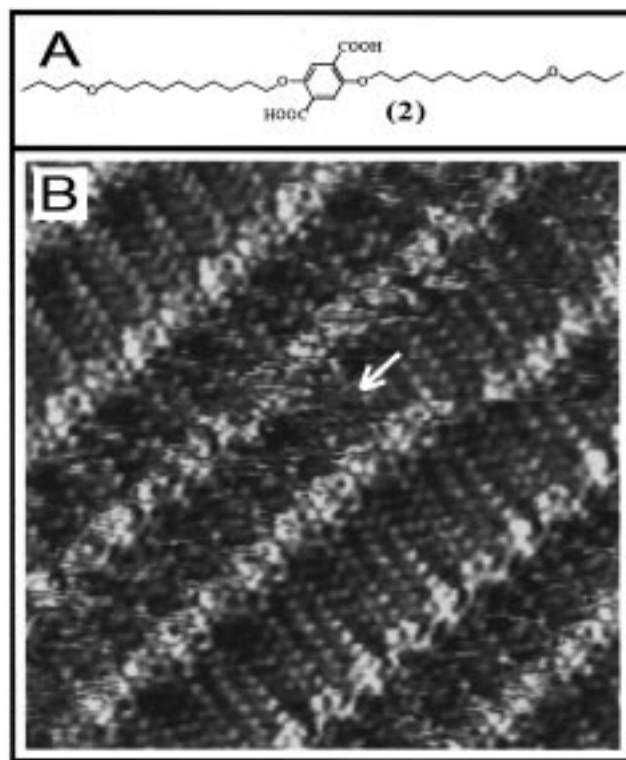


Figure 3. (A) Chemical structure of 2,5-bis[(10-butoxydecyl)-oxy]terephthalic acid (**2**). (B) STM image of a physisorbed monolayer of **2** at the 1-phenyloctane-graphite interface. Wide and narrow lamellae are still observed, as for monolayers of compound **1**. However, note the clear difference in image resolution between wide and narrow lamellae. The narrow lamellae appear more "noisy", because of the dangling butoxy groups which give rise to the horizontal streaks in the image. Within the wide lamellae, horizontal streaks are absent because **2** does not contain stereogenic centers. This leads to an enhancement of resolution in the wide lamellae. The image size is 9.5×9.5 nm². $I_{\text{set}} = 1.35$ nA, and $V_{\text{bias}} = -0.30$ V.

bent away from the graphite surface. The good agreement between our experimental value for the center to center distance and the value reported for this distance in a three-dimensional crystal indicates that neighboring terephthalic acid groups form hydrogen bonds.¹⁶ This suggests that, in addition to alkyl-alkyl and alkyl-substrate interactions, hydrogen bonding plays an important role in the two-dimensional organization.

The enantiomorphous monolayer formation is also expressed by the orientation of the monolayer with respect to the lattice of the underlying graphite surface. This was also observed for a chiral isophthalic acid derivative.⁹ Comparison of the direction of the lamellar axis, indicated by a white line in Figure 1B,C, of a (*S*)- or (*R*)-**1** domain with the underlying graphite substrate shows that this axis makes angles θ of respectively $-3.7 \pm 0.3^\circ$ and $+3.7 \pm 0.3^\circ$ (Figure 2B,C) with the normal on that particular graphite axis which is almost in registry with the alkoxy chains.¹⁸

In Figure 1D,E two high-resolution STM images of respectively (*S*)- and (*R*)-**1** monolayers are shown. In addition to the structural characteristics for these monolayers outlined above, these images reveal elongated discontinuous features, of which some are indicated by arrows. These features are observed in the narrow as well as in the wide lamellae. In the narrow lamellae, the position of those features can be identified with the location where we propose the 2-methylbutoxy groups to be pointing away from the graphite surface.

(13) Stevens, F.; Dyer, D. J.; Müller, U.; Walba, D. M. *Langmuir* **1996**, *12*, 5625–5629.

(14) Gorman, C. B.; Touzov, I.; Miller, R. *Langmuir* **1998**, *14*, 3052–3061.

(15) Stabel, A.; Heinz, R.; Rabe, J. P.; Wegner, G.; De Schryver, F. C.; Corens, D.; Dehaen, W.; Süling, C. *J. Phys. Chem.* **1995**, *99*, 8690–8697.

(16) Domenicano, M.; Schultz, G.; Hargittai, I.; Colapietro, M.; Portalone, G.; George, P. *Struct. Chem.* **1990**, *1*, 107.

(17) The cell parameters a , b , and γ of the unit cell of the wide lamellae measure respectively 0.96 ± 0.01 nm, 2.6 ± 0.1 nm, and $73 \pm 3^\circ$. The cell parameters a , b , and γ of the unit cell of the narrow lamellae measure respectively 0.96 ± 0.01 nm, 2.0 ± 0.1 nm, and $77 \pm 5^\circ$.

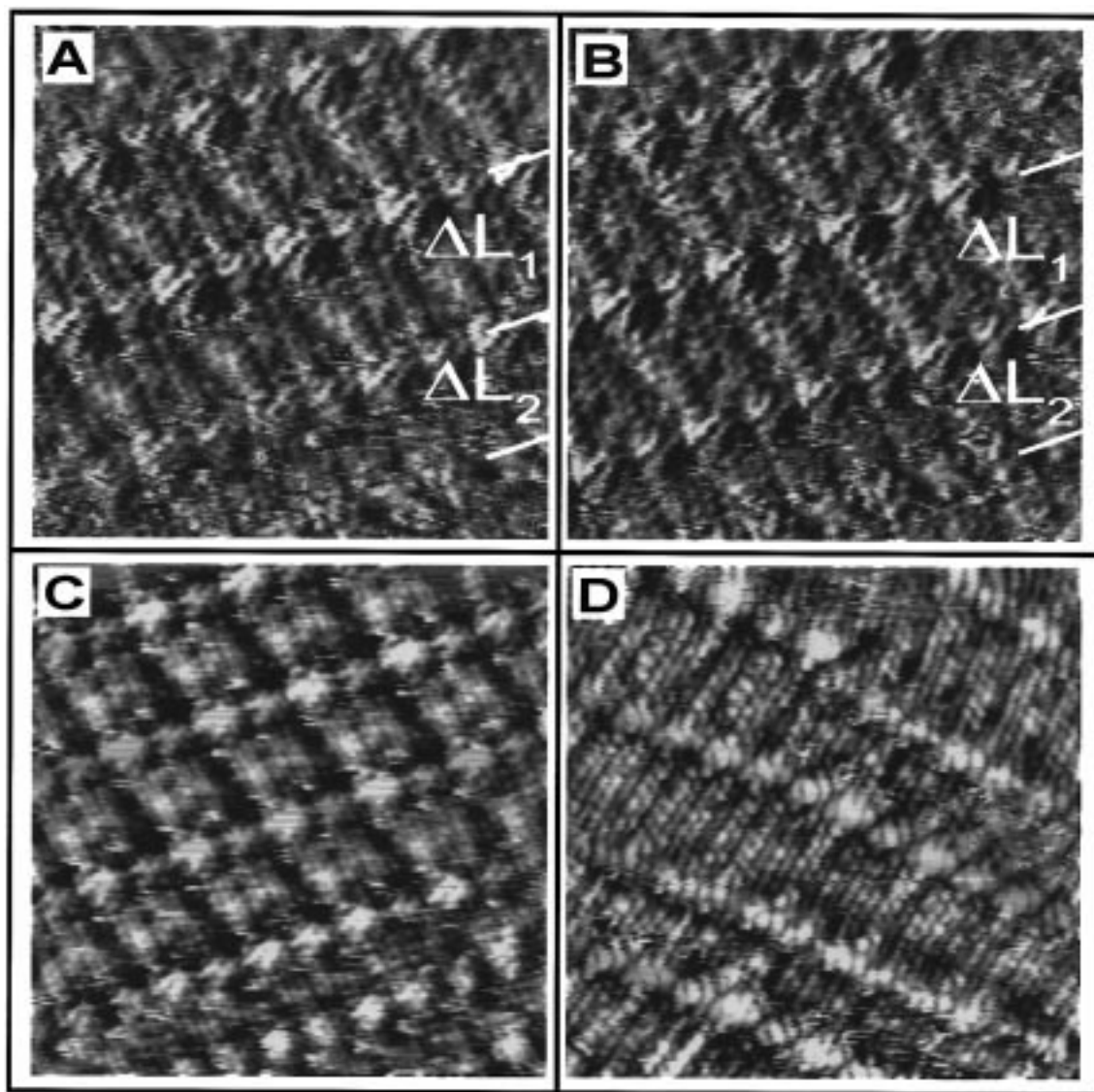


Figure 4. (A) STM image of a (*R*)-**1** monolayer at the 1-phenyloctane-graphite interface recorded at a bias voltage of -0.34 V. The image size is 8.2×8.2 nm². $I_{\text{set}} = 0.4$ nA. The wide and narrow lamellae are indicated by ΔL_1 and ΔL_2 , respectively. (B) STM image of a (*R*)-**1** monolayer recorded at a bias voltage of -0.52 V. The image size is 8.2×8.2 nm². $I_{\text{set}} = 0.4$ nA. The wide and narrow lamellae are indicated by ΔL_1 and ΔL_2 , respectively. Increasing the bias voltage leads to the disappearance of the spots in the wide lamellae correlated with the positions of the stereogenic centers. (C) Constant-current image of a (*R*)-**1** monolayer. The image size is 11.6×11.6 nm². $I_{\text{set}} = 0.3$ nA, and $V_{\text{bias}} = -0.35$ V. (D) Constant-current image of a monolayer of compound **2**. In constant-current mode streaky features identical to those visualized in constant-height mode can clearly be distinguished. In the wide lamellae of **2** no spots are visible. The image size is 9.8×9.8 nm². $I_{\text{set}} = 1.0$ nA, and $V_{\text{bias}} = -0.44$ V.

Apparently, the presence of the 2-methylbutoxy groups sticking out above the plain of the adsorbed monolayer results in a local alteration of the tunneling current. The discontinuous character of the observed features is probably related to the mobility of the nonadsorbed chain ends which interact with the STM tip during the scanning process.

However, these streaky features are also observed in the wide lamellae, in which the alkoxy chains are lying extended on the graphite surface. As was the case for the narrow lamellae, those spots are most likely caused by interaction between the scanning tip and the part of the molecule sticking out above the plain of the monolayer, in this instance the methyl unit on the tetrahedral stereogenic carbon atom, which is directed away from the graphite surface. To verify this hypothesis, STM images of a reference compound were recorded, namely, 2,5-bis-[(10-butoxydecyl)oxy]terephthalic acid (**2**) (Figure 3A), which has the same chemical structure as **1** except for the

methyl group at the chiral center. The compound was dissolved in 1-phenyloctane and adsorbed on the surface. As shown in Figure 3B, compound **2** also forms wide and narrow lamellae but only in the latter ones, in which the 1-butoxy groups are bent away from the surface, elongated features appear. This observation supports our hypothesis that the local change in tunneling current and loss of resolution in the wide lamellae of compound **1** is related to the presence of the methyl group at the stereogenic centers. This hypothesis is further supported by the observation that increasing the bias voltage, resulting in a slight retraction of the tip, leads to the disappearance of the spots correlated with the positions of the stereogenic centers, while the spots related to the 2-methylbutoxy groups are at the same voltage still visible. This means that, at larger distances between the tip and the graphite surface, only the butoxy group but not the methyl group interacts with the STM tip. This is shown in parts A and B of Figure 4, respectively.

In addition, constant-current mode measurements were performed in order to demonstrate that we can visualize identical structural features as detected in constant-height mode. Parts C and D of Figure 4 are constant-current STM images of (*R*)-**1** and **2**, respectively. In both images features corresponding to the short alkoxy chains bent away from the surface are clearly visible in the narrow lamellae. The wide lamellae of (*R*)-**1** also show features,

(18) Because the optical purity of the samples is not 100% (see the Experimental Section), it is not surprising that a small percentage of the observed lamellar orientations is not in agreement with the results outlined in the text. The main impurity in the samples is (*R,S*)-**1**. We assume that the methyl group on the stereogenic carbon atom of fully extended alkoxy chains is pointing away from the graphite surface, which is impossible for both alkoxy chains of (*R,S*)-**1** because of sterical interactions with the substrate. However, as mentioned above, the 2-methylbutoxy groups can be bent away from the surface. Therefore, we assume that those domains of which the sign of the angle θ deviates from the expected sign of the monolayer structures of the respective enantiomers are composed of (*R,S*)-**1**. Moreover, in these aberrant domains, two adjacent wide lamellae are never observed, which is in agreement with our model that both alkoxy chains of (*R,S*)-**1** cannot be fully extended. Those domains which reflect the two-dimensional organization of the (*S*)- or (*R*)-**1** enantiomers often show more than two adjacent wide lamellae (e.g., Figure 1C). It should be noted that (*R,S*)-**1** can also be included in narrow lamellae of domains composed of (*S*)- or (*R*)-**1**, with its fully extended alkoxy chain containing respectively a *S* or *R* center. Those eventually coadsorbed (*R,S*)-**1** molecules cannot be distinguished from the enantiomerically pure compounds. However, it can be concluded that all consecutive wide lamellae within a domain must consist of the pure (*S*)- or (*R*)-**1** enantiomer. The differences found between both enantiomers are in line with the optical purity of the compounds used.

now corresponding to the protruding methylene groups of the stereogenic centers, while in the wide lamellae of **2**, no streaky features are visible. These results are in agreement with the data obtained in the constant-height method.

Conclusions

In this paper, we have reported that the enantiomers of a chiral terephthalic acid derivative, carrying two stereogenic centers, form enantiomorphous monolayer structures. We have shown that monomolecular adlayers of chiral compounds can be imaged with submolecular resolution at the liquid-graphite interface and that it is possible to visualize the positions of small protruding groups in general and in particular to localize the stereogenic centers, due to the presence of a methyl group pointing away from the surface.

Acknowledgment. The authors thank FWO and DWTC for continuing financial support through IUAP-IV-11. S.D.F. is a postdoctoral fellow of the University of Leuven. A.G. thanks the IWT for a predoctoral scholarship. The collaboration was made possible in the context of the TMR network SISITOMAS.

LA9811057